Signatures of Dissipation Driven Quantum Phase Transition in Rabi Model

G. De Filippis[,1,2,*] A. de Candia[,1,2] G. Di Bello[,3] C. A. Perroni,[1] L. M. Cangemi[,4] A. Nocera,[5]
M. Sassetti,[6,7] R. Fazio[,1,8,9] and V. Cataudella[1,2]

[1]*SPIN-CNR and Dip. di Fisica E. Pancini—Università di Napoli Federico II—I-80126 Napoli, Italy*
[2]*INFN, Sezione di Napoli—Complesso Universitario di Monte S. Angelo—I-80126 Napoli, Italy*
[3]*Dipartimento di Fisica Ettore Pancini—Università di Napoli Federico II—I-80126 Napoli, Italy*
[4]*Department of Chemistry, Bar-Ilan University, Ramat-Gan 52900, Israel*
[5]*Department of Physics and Astronomy and Stewart Blusson Quantum Matter Institute, University of British Columbia,
Vancouver, British Columbia, Canada, V6T 1Z1*
[6]*Dipartimento di Fisica, Università di Genova, I-16146 Genova, Italy*
[7]*SPIN-CNR, I-16146 Genova, Italy*
[8]*ICTP, Strada Costiera 11, I-34151 Trieste, Italy*
[9]*NEST, Istituto Nanoscienze-CNR, I-56126 Pisa, Italy*

By using the worldline Monte Carlo technique, matrix product state, and a variational approach *à la* Feynman, we investigate the equilibrium properties and relaxation features of the dissipative quantum Rabi model, where a two level system is coupled to a linear harmonic oscillator embedded in a viscous fluid. We show that, in the Ohmic regime, a Beretzinski-Kosterlitz-Thouless quantum phase transition occurs by varying the coupling strength between the two level system and the oscillator. This is a nonperturbative result, occurring even for extremely low dissipation magnitude. By using state-of-the-art theoretical methods, we unveil the features of the relaxation towards the thermodynamic equilibrium, pointing out the signatures of quantum phase transition both in the time and frequency domains. We prove that, for low and moderate values of the dissipation, the quantum phase transition occurs in the deep strong coupling regime. We propose to realize this model by coupling a flux qubit and a damped LC oscillator.

In 1936 Rabi introduced a model describing the simplest class of light-matter interaction, i.e., the dipolar coupling between a two-level quantum system (qubit) and a classical monochromatic radiation field (unidimensional harmonic oscillator) [1]. In its quantum version [2–4], i.e., the so-called quantum Rabi model, the radiation is specified by a quantized single-mode field. In general, the interaction between an atom and the electromagnetic field inside a cavity allows us to get not only a deep understanding of the light-matter interaction, but it also plays a significant role in different quantum technologies, including lasers and many quantum computing architectures [5,6] like ultrafast gates [7], quantum error correcting codes [8], remote entanglement generation [9], cold atoms, and trapped ions [10]. Recently, the coherent coupling of a single photon mode and a superconducting charge qubit has been extensively studied both from theoretical [11–15] and experimental points of view [16–20]. Nowadays, the realization of strong, ultrastrong, and deep strong coupling [21,22] between artificial atoms and cavities is possible, for instance, by inductively coupling a flux qubit and an LC oscillator via Josephson junctions [20]. Indeed, an important feature of the flux qubit is its strong anharmonicity: the two lowest energy levels are well isolated from the higher

levels. In the most interesting regime, the deep strong coupling one, where the coupling strength becomes as large as the atomic and cavity frequencies, the energy eigenstates of the qubit-resonator system are highly entangled. On the other hand, one of the central problems is the full understanding of all the physical properties of such quantum systems when the interaction with environmental degrees of freedom, inducing decoherence and dissipation, is explicitly taken into account. Specifically, the questions we want to address in the present Letter are does the dissipative quantum Rabi model exhibit a quantum phase transition (QPT), and what is its signature in linear response measurements?

In the literature the existence of a QPT has been addressed in the Dicke model [23–26] and the resistively shunted Josephson junction [27–31]. In the former case, describing a collection of N two-level atoms interacting with a single bosonic mode via a dipole interaction, it has been proved that the system undergoes a transition from quasi-integrability to quantum chaos, and that this transition is caused by the precursors of the QPT, occurring when $N \to \infty$. In the latter case, where a Josephson junction and its capacitor, analogous to a massive particle in a washboard potential, are coupled to a bath of harmonic

oscillators that provides viscous damping, the existence of a QPT has given rise to a long-standing controversy [27]. Indeed, the absence of QPT, in the parameter regime predicted theoretically, has been reported [27]. In a simpler case, the spin-boson model, where a system with only two energy levels is coupled to an Ohmic environment, QPT existence has been well established [32]. Indeed, by increasing the interaction between the qubit and the bath, QPT occurs.

Recently it has been shown that the Rabi Hamiltonian exhibits a QPT despite consisting only of a single-mode cavity field and a two-level atom [33,34]. It appears when the cavity frequency ω_0, in units of the qubit gap Δ, tends to zero, i.e., QPT takes place in the classical limit for the harmonic oscillator. In particular, it has been proved that (i) the number of spins in the Dicke model and the ratio Δ/ω_0 in the Rabi model play an identical role and (ii) the open Rabi model exhibits a mean field second-order dissipative phase transition [35]. These predictions have been experimentally observed [36].

In this Letter, we show that in the fully quantum limit, i.e., $\omega_0/\Delta \neq 0$, the dissipative Rabi model exhibits another and completely different QPT: by increasing the qubit-resonator interaction a Beretzinski-Kosterlitz-Thouless (BKT) QPT occurs. In particular, we prove that this is a not perturbative result. Indeed, QPT takes place for any fixed, but nonvanishing, value of the coupling between the cavity and the bath. First, by using the worldline Monte Carlo (WLMC) method [37–39], based on the path integrals, and a variational approach à la Feynman [37–39,50], we investigate the equilibrium properties of the dissipative quantum Rabi model. We prove that, in the Ohmic regime, a BKT QPT occurs by varying the coupling strength between the two level system and the oscillator, even for extremely low dissipation magnitude. In particular, by indicating with α_{cav} the strength of the coupling between the cavity and the bosonic bath, we show that QPT sets in when $4g^2\alpha_{\mathrm{cav}} \simeq \omega_0^2$, i.e., for low and moderate values of the dissipation, $\alpha_{\mathrm{cav}} \lesssim 0.25$, QPT occurs in the deep strong coupling regime that, nowadays, can be experimentally reached. Furthermore, by using matrix product state simulations (MPS) [39,51–55], and combining the Mori formalism [39,56] and a variational approach à la Feynman, we investigate also the relaxation processes towards the thermodynamic equilibrium. They allow us to identify the signatures of the QPT both in the time and frequency domains, establishing a relation between the order parameter and a typical linear response measurement like the magnetic susceptibility.

The model.—The Hamiltonian is written as

$$H = H_{Q-O} + H_I, \tag{1}$$

where (i) $H_{Q-O} = -(\Delta/2)\sigma_x + \omega_0 a^\dagger a + g\sigma_z(a + a^\dagger)$ describes the qubit-oscillator system, Δ being the tunneling

matrix element, a ($a^\dagger$) standing for the annihilation (creation) operator for the bosonic field with frequency ω_0, and g representing the strength of the coupling and (ii) $H_I = \sum_{i=1}^{N} [(p_i^2/2M_i) + (k_i/2)(x - x_i)^2]$ describes the environmental degrees of freedom and their interaction with the resonator. The bath is represented as a collection of harmonic oscillators with frequencies $\omega_i^2 = (k_i/M_i)$, and coordinates and momenta given by x_i and p_i, respectively; furthermore, x denotes the position operator of the resonator with mass m: $x = \sqrt{(1/2m\omega_0)}(a + a^\dagger)$. Units are such that $\hbar = k_B = 1$. We emphasize that, in Eq. (1), σ_x and σ_z are Pauli matrices with eigenvalues 1 and −1. The dissipative environment is modeled as a strictly Ohmic bath with spectral density: $J(\omega) = \sum_{i=1}^{N}(k_i\omega_i/2m\omega_0)\delta(\omega - \omega_i) = \alpha_{\mathrm{cav}}\omega\theta(\omega_c - \omega)$. Here the adimensional parameter α_{cav} measures the strength of the coupling and ω_c is a cutoff frequency. By means of the unitary transformation that diagonalizes the Hamiltonian of the cavity and its environment, the model can be mapped [12,14,39] to the Hamiltonian of a single two level system, with gap Δ, interacting, through σ_z operator, with a structured bosonic bath. The effective spectral density function, $J_{\mathrm{eff}}(\omega) = \sum_{i=1}^{N+1} l_i^2\delta(\omega - \tilde{\omega}_i)$, is given by

$$J_{\mathrm{eff}}(\omega) = \frac{2g^2\omega_0^2\alpha_{\mathrm{cav}}\omega\theta(\omega_c - \omega)}{[\omega^2 - \omega_0^2 - h(\omega)]^2 + (\pi\alpha_{\mathrm{cav}}\omega_0\omega)^2}, \tag{2}$$

$\tilde{\omega}_i$ being the frequencies of the $N + 1$ bosonic normal modes stemming from the diagonalization of the cavity-environment Hamiltonian, l_i the couplings with σ_z, and $h(\omega) = \alpha_{\mathrm{cav}}\omega_0\omega \log[(\omega_c + \omega)/(\omega_c - \omega)]$. We emphasize that $J_{\mathrm{eff}}(\omega)$ features a Lorentzian peak at the oscillator frequency ω_0 with width $\pi\alpha_{\mathrm{cav}}\omega_0$, and, at low frequencies, $\omega \ll \omega_0$, exhibits an Ohmic behavior, $J_{\mathrm{eff}}(\omega) \simeq (\alpha_{\mathrm{eff}}/2)\omega$, with $\alpha_{\mathrm{eff}} = 4g^2\alpha_{\mathrm{cav}}/\omega_0^2$. In the following we set $\alpha_{\mathrm{cav}} = 0.2$, $\omega_0 = 0.75\Delta$, and $\omega_c = 10\Delta$.

QPT evidences at the thermodynamic equilibrium.—We investigate the equilibrium properties by using two different approaches. The first one is a variational approach à la Feynman at finite temperature [37–39]. The other one is WLMC method, based on the path integrals [37–39]. Here the elimination of the structured bath degrees of freedom leads to an effective Euclidean action [32,39,57,58]:

$$S = \frac{1}{2}\int_0^\beta d\tau \int_0^\beta d\tau' \sigma_z(\tau)K_{\mathrm{eff}}(\tau - \tau')\sigma_z(\tau'), \tag{3}$$

where $\beta = 1/T$ (T is the system temperature), and the kernel is expressed in terms of the spectral density $J_{\mathrm{eff}}(\omega)$ and the bath propagator: $K_{\mathrm{eff}}(\tau) = \int_0^\infty d\omega J_{\mathrm{eff}}(\omega)\{\cosh[\omega(\beta/2 - \tau)]/\sinh(\beta\omega/2)\}$. The problem turns out to be equivalent to a classical system of spin variables distributed on a chain with length β, and
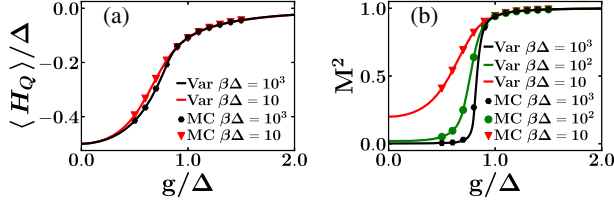
FIG. 1. $\langle H_Q \rangle/\Delta$ (a) and M^2 (b) vs g/Δ at different temperatures: comparison between WLMC method and the variational approach (MC and Var in the figure).

ferromagnetically interacting with each other with strength $K_{\text{eff}}(\tau - \tau')$ (τ and τ' label the spins on the chain). The functional integral is done with Poissonian measure adopting a cluster algorithm [57,59], based on the Swendsen-Wang approach [39,60]. In particular, if ω_0 is kept constant and $\beta \to \infty$, K_{eff} has the asymptotic behavior: $K_{\text{eff}}(\tau) = (\alpha_{\text{eff}}/2\tau^2)$. We will prove that it determines the onset of a BKT QPT.

In Fig. 1 we plot $\langle H_Q \rangle$, in units of Δ, with $H_Q = -(\Delta/2)\sigma_x$, i.e., the two-level system Hamiltonian, and qubit squared magnetization, $M^2 = (1/\beta)\int_0^\beta d\tau \langle \sigma_z(\tau)\sigma_z(0)\rangle$, as a function of g/Δ, for different temperatures, from $T = 10^{-1}\Delta$ to $T = 10^{-3}\Delta$. The plots point out the successful agreement between the two proposed approaches. As expected, by increasing g/Δ, $\langle H_Q \rangle$ increases, indicating a progressive reduction of the effective tunneling. Interestingly, we emphasize that $\langle H_Q \rangle$ is always different from zero, even for extremely large values of g/Δ, and slightly depends on the temperature.

On the other hand, M^2 increases from 0 to about 1, in a steeper and steeper way by lowering T, signaling an incipient QPT, that is a BKT QPT. Indeed, in a BKT transition, the quantity M^2 should exhibit a discontinuity at a critical value of g/Δ and $T = 0$ [61,62]. In order to get a precise estimation of the critical value of the coupling, i.e., g_c, and then critical value of α_{eff}, i.e., α_c, we adapt the approach suggested by Minnhagen *et al.* in the framework of the XY model [63–65]. In the present context, the roles of the chirality and the lattice size are played by squared magnetization and inverse temperature β, respectively. Defining the scaled order parameter $\Psi(\alpha_{\text{eff}}, \beta) = \alpha_{\text{eff}}M^2$, the BKT theory predicts for large values of β, i.e., asymptotically: $[\Psi(\alpha_c, \beta)]/(\Psi_c) = 1 + [1/2(\ln\beta - \ln\beta_0)]$, where β_0 is the only fitting parameter and $\Psi_c = \Psi(\alpha_c, \beta \to \infty)$ is the universal jump that is expected to be equal to 1. In this scenario, the function $G(\alpha_{\text{eff}}, \beta) = [1/\Psi(\alpha_{\text{eff}}, \beta) - 1] - 2\ln\beta$ should not show any dependence on β at $\alpha_{\text{eff}} = \alpha_c$. In Fig. 2(a) we plot the function $G(\alpha_{\text{eff}}, \beta)$, as a function of β, for different values of g/Δ, and then α_{eff}. The plots clearly show that there is a value of α_{eff} such that G is independent on β asymptotically. This determines α_c. In the presence of a purely Ohmic bath, i.e., $J(\omega) = (\alpha/2)\omega\Theta(\omega_c - \omega)$, the critical value of α is about
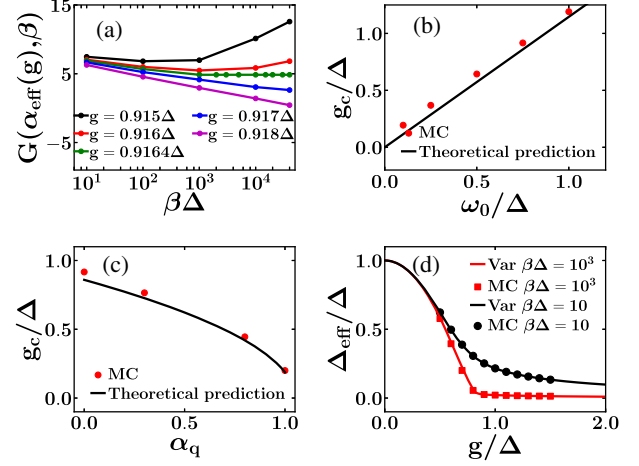

FIG. 2. (a) The function G vs $\beta\Delta$ at $g \simeq g_c$ by using WLMC technique; g_c/Δ vs ω_0/Δ (b) and α_q (c) comparison between WLMC method and an effective theory based only on the low frequency contribution of the spectral density [$\omega_0/\Delta = 0.75$ in (c)]; (d) the qubit effective gap at two different temperatures: comparison between WLMC technique and variational approach (MC and Var in the figure).

1.05 at $\omega_c = 10\Delta$ [37]. In Fig. 2(b) we plot g_c/Δ vs ω_0/Δ compared with that obtained by taking into account only the low-frequency contribution of the spectral density function, i.e., by imposing $\alpha_c = 4g_c^2\alpha_{\text{cav}}/\omega_0^2 = 1.05$. The successful agreement clearly shows that QPT is driven by the asymptotic behavior of the spectral density, i.e., by the long range interaction of the mapped spin system that decays as $1/\tau^2$. In order to further corroborate this observation, we take into account also the direct influence of the environment on the qubit, i.e., we add another contribution in the spectral density function of Eq. (2): $(\alpha_q/2)\omega\Theta(\omega_c - \omega)$. It stems from the interaction between an Ohmic bath and the qubit through the operator σ_z. In Fig. 2(c) we compare g_c/Δ vs α_q, computed by means of MC technique at $\omega_0/\Delta = 0.75$, with that obtained by retaining only the low-frequency contribution in the bath spectral density, i.e., by imposing $\alpha_q + \alpha_{\text{eff}} = 1.05$. The plot, also in this case, points out the robustness of the previously discussed hypothesis. It is worth noting that the equation determining the QPT onset, i.e., $\alpha_c = 4g_c^2\alpha_{\text{cav}}/\omega_0^2 = 1.05$, proves that, for $\alpha_{\text{cav}} \lesssim 0.25$, the quantum transition occurs in the deep strong coupling regime. We also emphasize that, within the BKT QPT scenario, i.e., ω_0 is finite and $\beta \to \infty$, g_c is proportional to ω_0. On the other hand, when $\omega_0 \to 0$ and $\beta \to \infty$, with $\omega_0\beta \to 0$, the kernel in Eq. (3) is independent of τ, so that a mean field transition occurs [33,34,39]. It is controlled by the adimensional parameter $\lambda = (g^2/\omega_0\Delta)$ with $\lambda_c = \frac{1}{4}$, i.e., $g_c \propto \sqrt{\omega_0}$. In the Supplemental Material [39] we also investigate the physical consequences on the resonator of the BKT QPT occurrence. Starting from the resonator

Green's function, $D(\tau)$, relative to resonator position operator x, we find an exact relation between $X^2 = (1/\beta) \int_0^\beta d\tau \langle x(\tau) x(0) \rangle$ and M^2. We prove that both these physical quantities exhibit a discontinuity in the BKT QPT, whereas they increase linearly with $\lambda - \lambda_c$ in the mean field transition [39].

QPT evidences from relaxation function and magnetic susceptibility.—Let us suppose that the system at $t = -\infty$ is at the thermal equilibrium. The response of the system to a perturbation, adiabatically applied from $t = -\infty$ and cutoff at $t = 0$, can be calculated within the Mori formalism and the linear response theory [66]. In particular, in the presence of a small magnetic field h along the z axis, $\forall\ t \geq 0$ the most important physical quantity is the qubit relaxation function $\Sigma_z(t) = (\langle \sigma_z(t) \rangle / \langle \sigma_z(0) \rangle)$ (calculated in the absence of h, being $t \geq 0$). Within the Mori formalism [39,56], where the inner product between two operators is defined by $(A, B) = (1/\beta) \int_0^\beta \langle e^{sH} A^\dagger e^{-sH} B \rangle ds$, it is possible to prove that $\Sigma_z(t) = \{[\sigma_z(0), \sigma_z(t)] / [\sigma_z(0), \sigma_z(0)]\}$.

Furthermore $\Sigma_z(z)$, the Laplace-transformed relaxation function, is strictly related to the magnetic susceptibility $\chi(z) = -i \int_0^\infty e^{izt} \langle [\sigma_z(t), \sigma_z(0)] \rangle dt$, where z lies in the complex upper half plane, i.e., $z = \omega + i\epsilon$, with $\epsilon > 0$. Indeed, $\Sigma_z(z) = i\{[\chi(z) - \chi(z=0)] / M^2 \beta z\}$, that is the analog of the relation between the optical conductivity and the current-current correlation function in solids [67]. By using the eigenbasis of the interacting system Hamiltonian and the commutation relation $[\sigma_z, H] = -i\Delta \sigma_y$, it is straightforward to deduce the following two very interesting properties:

$$M^2 \beta = -\frac{2}{\pi} \int_0^\infty \frac{\mathfrak{I}[\chi(\omega)]}{\omega} d\omega, \qquad (4)$$

and

$$\Sigma_z(z) = \frac{i}{z} + \frac{(\sigma_y, \sigma_y)}{(\sigma_z, \sigma_z)} \Delta^2 \Sigma_y(z). \qquad (5)$$

Equation (4) shows that the behavior of the magnetic susceptibility at low frequencies is directly related to the order parameter of QPT. Note that $M^2 \beta$, when $\beta \to \infty$, tends to a finite constant depending on g for $g < g_c$, whereas, at $g \geq g_c$, diverges. On the other hand, Eq. (5), which establishes a connection between $\Sigma_z(z)$ and $\Sigma_y(z)$, i.e., between the two relaxation functions along z and y axes, allows us to define an effective gap: $\Delta_{\text{eff}}^2 = [(\sigma_y, \sigma_y) / (\sigma_z, \sigma_z)] \Delta^2$. In particular it restores the bare qubit gap Δ at $g = 0 = \alpha_{\text{cav}}$. In Fig. 2(d) we plot the effective gap, in units of Δ, as function of g/Δ at two different temperatures. We emphasize that this important physical quantity provides a precise indication of the onset of QPT, being related to M^2. Indeed $(\sigma_z, \sigma_z) = M^2$ and $(\sigma_y, \sigma_y) = (2\langle \sigma_x \rangle / \beta \Delta)$. It is worth noticing that simple, but not

accurate, variational approaches, based on polaronic unitary transformations [12], provide a discontinuity in the quantity $\langle H_Q \rangle$ that is generally associated to the onset of QPT. We highlight that this jump is an artifact of this kind of approximate methods, indeed it is present neither in WLMC technique nor the variational approach *à la* Feynman as previously discussed. It confirms that Δ_{eff}, and then M^2, and not $\langle H_Q \rangle$ represents the right order parameter of QPT.

In a previous paper [38,67] we have proved that $\Sigma_y(z)$ can be exactly expressed in terms of a weighted sum contributions associated to the eigenstates of the interacting system, each characterized by its own frequency-dependent relaxation time:

$$\Sigma_y(z) = \sum_n P_n \frac{i}{z + iM_n(z)}, \qquad (6)$$

with $\sum_n P_n = 1$. We emphasize that so far there is no approximation. Here, we combine, for the calculation of $\Sigma_y(z)$, the short-time approximation, typical of the memory function formalism [56], and the approach *à la* Feynman, by replacing, in $M_n(z)$, the exact eigenstates of H with the ones of H_M, whose parameters are variationally determined. Indeed, since the commutator between σ_y and H involves a contribution proportional to the qubit-boson coupling, the short-time approximation can be more easily implemented for the calculation of the relaxation function $\Sigma_y(z)$ [38]. Once $\Sigma_y(z)$ is known, Eq. (5) allows us to obtain $\Sigma_z(t)$. In Fig. 3 we compare $\Sigma_z(t)$ with that obtained through MPS approach [39], where a standard matrix product operator representation of the time evolution operator $U(t + dt, t) = \exp(-iHdt)$ [52] is implemented using the ITensor library [54]. This method allows us to simulate the non-equilibrium dynamics of long-ranged model Hamiltonians starting from a generic initial state. In our case the initial state is the ground state of H in the presence of a small magnetic field along z axis, as previously discussed.

The plots in Fig. 3 show that, at weak coupling, the dynamics is characterized by Rabi oscillations, whose amplitude and frequency reduce by increasing the strength of the coupling g/Δ. By further increasing g/Δ, the relaxation becomes exponential: this is the analog of the Toulouse point in the spin-boson model. Then the relaxation time gets longer and longer, and, at $g \geq g_c$, the system does not relax, i.e., $\Sigma_z(t) = 1$ independently on time t, signaling the occurrence of QPT. The behavior of the relaxation function in the frequency domain sheds further light on the relaxation processes. In the weak coupling regime, the real part of $\Sigma_z(\omega)$ exhibits only a peak centered, essentially, at the bare qubit gap Δ. At $g = 0.28\Delta$, the effective gap turns out to be equal to the resonator frequency: the spectrum presents avoided crossings, giving rise to the so called vacuum Rabi splitting [68]. By
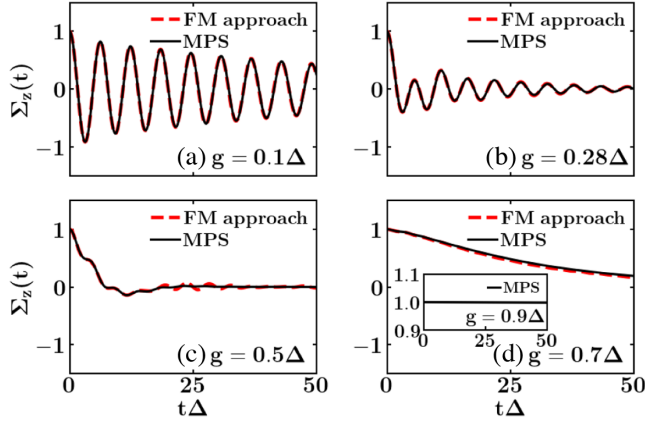
FIG. 3. $\Sigma_z(t)$ at different values of g/Δ: comparison between the Feynman-Mori (FM) approach ($\beta\Delta = 5000$) and MPS method ($T = 0$). In the inset of panel (d) MPS simulation at $g \simeq g_c$, where there is no relaxation.

increasing g/Δ, there is a transfer of spectral weight towards lower frequencies. In particular, when $\Sigma_z(t)$ exhibits an exponential behavior, $\Re[\Sigma_z(\omega)]$ is characterized by a peak centered at zero frequency. As shown in Fig. 4, the width of this structure becomes narrower and narrower, and, at $g = g_c$, $\Re[\Sigma_z(\omega)]$ exhibits a delta function centered at zero frequency: it signals the onset of QPT.

Starting from an inductive coupling between a flux qubit and an LC oscillator via Josephson junctions as in [20], for the experimental observation we propose to introduce a dissipative element in the LC circuit. Following Devoret [69,70] we replace it with a continuum of harmonic oscillators as in the Caldeira-Legget model [71]. By using the values measured in Ref. [20], the resistance turns out to be $R \simeq (0.24/\alpha_{cav})\ k\Omega$, so that $\alpha_{cav} \simeq 0.2$ corresponds to $R \simeq 1.2\ k\Omega$. Then, for moderate values of the dissipation, R is of the order of $k\Omega$ and QPT occurs for values of $g_c/\omega_0 \simeq 1$, i.e., g_c lies in the deep strong coupling regime that can be experimentally reached [20].
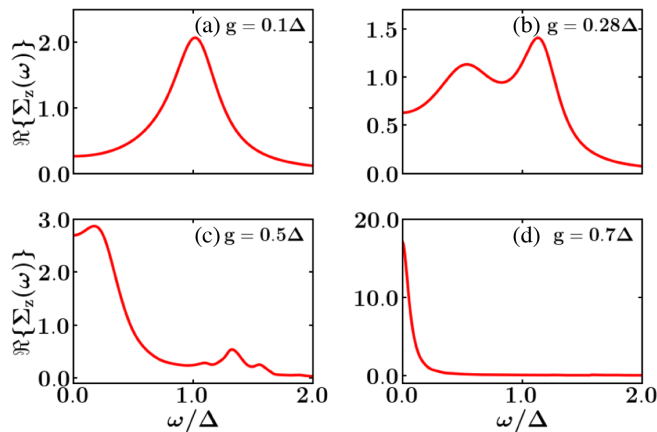

FIG. 4. $\Sigma_z(\omega)$ at different values of g/Δ within Feynman-Mori approach ($\beta\Delta = 5000$).

Conclusions.—We proved that the open quantum Rabi model exhibits a QPT by varying the strength of the coupling between the qubit and the resonator, even in the presence of extremely low dissipation magnitude. We characterized QPT unveiling its signatures both at and out of thermodynamic equilibrium by using typical linear response measurements.

*Corresponding author.
giulio.defilippis@unina.it
[1] I. I. Rabi, Phys. Rev. **49**, 324 (1936).
[2] E. Jaynes and F. Cummings, Proc. IEEE **51**, 89 (1963).
[3] D. Zueco, G. M. Reuther, S. Kohler, and P. Hänggi, Phys. Rev. A **80**, 033846 (2009).
[4] D. Braak, Phys. Rev. Lett. **107**, 100401 (2011).
[5] J. M. Raimond, M. Brune, and S. Haroche, Rev. Mod. Phys. **73**, 565 (2001).
[6] H. Mabuchi and A. C. Doherty, Science **298**, 1372 (2002).
[7] G. Romero, D. Ballester, Y. M. Wang, V. Scarani, and E. Solano, Phys. Rev. Lett. **108**, 120501 (2012).
[8] T. H. Kyaw, D. A. Herrera-Martí, E. Solano, G. Romero, and L.-C. Kwek, Phys. Rev. B **91**, 064503 (2015).
[9] S. Felicetti, M. Sanz, L. Lamata, G. Romero, G. Johansson, P. Delsing, and E. Solano, Phys. Rev. Lett. **113**, 093602 (2014).
[10] D. Leibfried, R. Blatt, C. Monroe, and D. Wineland, Rev. Mod. Phys. **75**, 281 (2003).
[11] D. Z. Rossatto, C. J. Villas-Bôas, M. Sanz, and E. Solano, Phys. Rev. A **96**, 013849 (2017).
[12] D. Zueco and J. García-Ripoll, Phys. Rev. A **99**, 013807 (2019).
[13] L. Magazzù and M. Grifoni, J. Stat. Mech. (2019) 104002.
[14] M. C. Goorden, M. Thorwart, and M. Grifoni, Phys. Rev. Lett. **93**, 267005 (2004).
[15] J. Larson and T. Mavrogordatos, *The Jaynes-Cummings Model and Its Descendants* (IOP Publishing, 2021), pp. 2053–2563.
[16] I. Chiorescu, P. Bertet, K. Semba, Y. Nakamura, C. J. P. M. Harmans, and J. E. Mooij, Nature (London) **431**, 159 (2004).
[17] A. Wallraff, D. I. Schuster, A. Blais, L. Frunzio, R.-S. Huang, J. Majer, S. Kumar, S. M. Girvin, and R. J. Schoelkopf, Nature (London) **431**, 162 (2004).
[18] T. Niemczyk, F. Deppe, H. Huebl, E. P. Menzel, F. Hocke, M. J. Schwarz, J. J. Garcia-Ripoll, D. Zueco, T. Hümmer, E. Solano, A. Marx, and R. Gross, Nat. Phys. **6**, 772 (2010).
[19] P. Forn-Díaz, J. Lisenfeld, D. Marcos, J. J. García-Ripoll, E. Solano, C. J. P. M. Harmans, and J. E. Mooij, Phys. Rev. Lett. **105**, 237001 (2010).

[20] F. Yoshihara, T. Fuse, S. Ashhab, K. Kakuyanagi, S. Saito, and K. Semba, Nat. Phys. **13**, 44 (2017).

[21] G. Wendin, Rep. Prog. Phys. **80**, 106001 (2017).

[22] In general, the strong coupling regime is obtained when g exceeds the rate at which excitations decay into the environment, g being the strength of the coupling qubit resonator. If g is small with respect to the resonator frequency ω_0 and the qubit gap Δ, and the frequencies fulfill the condition $|\Delta - \omega_0| \ll |\omega_0 + \Delta|$, the interaction is faithfully described with the Jaynes-Cummings model, where coupling terms that simultaneously excite or deexcite the system and the field are neglected. When g/Δ and g/ω_0 are about 0.1, the Jaynes-Cummings model fails in rightly describing the Rabi model: This is the so-called strong coupling regime. Finally if g/Δ and g/ω_0 are of order of 1 or greater than 1, the deep strong coupling regime is reached.

[23] C. Emary and T. Brandes, Phys. Rev. E **67**, 066203 (2003).

[24] T. Jaako, Z.-L. Xiang, J. J. Garcia-Ripoll, and P. Rabl, Phys. Rev. A **94**, 033850 (2016).

[25] M. Bamba and N. Imoto, Phys. Rev. A **96**, 053857 (2017).

[26] A. Baksic and C. Ciuti, Phys. Rev. Lett. **112**, 173601 (2014).

[27] A. Murani, N. Bourlet, H. le Sueur, F. Portier, C. Altimiras, D. Esteve, H. Grabert, J. Stockburger, J. Ankerhold, and P. Joyez, Phys. Rev. X **10**, 021003 (2020).

[28] F. Guinea, V. Hakim, and A. Muramatsu, Phys. Rev. Lett. **54**, 263 (1985).

[29] P. Werner and M. Troyer, Phys. Rev. Lett. **95**, 060201 (2005).

[30] S. L. Lukyanov and P. Werner, J. Stat. Mech. (2007) P06002.

[31] K. Masuki, H. Sudo, M. Oshikawa, and Y. Ashida, Phys. Rev. Lett. **129**, 087001 (2022).

[32] U. Weiss, *Quantum Dissipative Systems* (World Scientific, Singapore, 1999).

[33] M.-J. Hwang, R. Puebla, and M. B. Plenio, Phys. Rev. Lett. **115**, 180404 (2015).

[34] S. Ashhab, Phys. Rev. A **87**, 013826 (2013).

[35] M.-J. Hwang, P. Rabl, and M. B. Plenio, Phys. Rev. A **97**, 013825 (2018).

[36] M.-L. Cai, Z.-D. Liu, W.-D. Zhao, Y.-K. Wu, Q.-X. Mei, Y. Jiang, L. He, X. Zhang, Z.-C. Zhou, and L.-M. Duan, Nat. Commun. **12**, 1126 (2021).

[37] G. De Filippis, A. de Candia, L. M. Cangemi, M. Sassetti, R. Fazio, and V. Cataudella, Phys. Rev. B **101**, 180408(R) (2020).

[38] G. De Filippis, A. de Candia, A. S. Mishchenko, L. M. Cangemi, A. Nocera, P. A. Mishchenko, M. Sassetti, R. Fazio, N. Nagaosa, and V. Cataudella, Phys. Rev. B **104**, L060410 (2021).

[39] See Supplemental Material at http://link.aps.org/supplemental/10.1103/PhysRevLett.130.210404 for more details on the model and the approaches used in the main text, a discussion on the two phase transitions occurring in the dissipative Rabi model, and an investigation of the physical consequences on the resonator in the case of the BKT QPT occurrence. Supplemental Material includes Refs. [40–49]. We also calculate the resonator mean phonon number $\langle a^\dagger a \rangle$ and prove that it does not show any singular behavior at g_c when BKT QPT takes place, whereas, in the mean field transition, it is zero for $\lambda < \lambda_c$ and diverges at λ_c. Finally, we demonstrate that mean field transition is independent on the coupling strength with the environment, whereas BKT QPT is induced by the interaction with the heat bath. All these observations prove that the two phase transitions occurring in the Rabi model are completely different.

[40] J. Haegeman, J. I. Cirac, T. J. Osborne, I. Pižorn, H. Verschelde, and F. Verstraete, Phys. Rev. Lett. **107**, 070601 (2011).

[41] J. Haegeman, C. Lubich, I. Oseledets, B. Vandereycken, and F. Verstraete, Phys. Rev. B **94**, 165116 (2016).

[42] C. Zhang, E. Jeckelmann, and S. R. White, Phys. Rev. Lett. **80**, 2661 (1998).

[43] R. J. Bursill, Phys. Rev. B **60**, 1643 (1999).

[44] B. Friedman, Phys. Rev. B **61**, 6701 (2000).

[45] H. Wong and Z.-D. Chen, Phys. Rev. B **77**, 174305 (2008).

[46] C. Brockt, F. Dorfner, L. Vidmar, F. Heidrich-Meisner, and E. Jeckelmann, Phys. Rev. B **92**, 241106(R) (2015).

[47] D. Jansen, J. Bonča, and F. Heidrich-Meisner, Phys. Rev. B **106**, 155129 (2022).

[48] R. P. Feynman, Phys. Rev. **84**, 108 (1951).

[49] K. T. Liu, D. N. Beratan, and P. Zhang, Phys. Rev. A **105**, 032406 (2022).

[50] R. P. Feynman, Phys. Rev. **97**, 660 (1955).

[51] S. R. White and A. E. Feiguin, Phys. Rev. Lett. **93**, 076401 (2004).

[52] M. P. Zaletel, R. S. K. Mong, C. Karrasch, J. E. Moore, and F. Pollmann, Phys. Rev. B **91**, 165112 (2015).

[53] S. Paeckel, T. Köhler, A. Swoboda, S. R. Manmana, U. Schollwöck, and C. Hubig, Ann. Phys. (Amsterdam) **411**, 167998 (2019).

[54] M. Fishman, S. R. White, and E. M. Stoudenmire, SciPost Phys. Codebases **4** (2022).

[55] A. W. Chin, A. Rivas, S. F. Huelga, and M. B. Plenio, J. Math. Phys. (N.Y.) **51**, 092109 (2010).

[56] H. Mori, Prog. Theor. Phys. **34**, 399 (1965).

[57] A. Winter, H. Rieger, M. Vojta, and R. Bulla, Phys. Rev. Lett. **102**, 030601 (2009).

[58] R. P. Feynman, Phys. Rev. **80**, 440 (1950).

[59] H. Rieger and N. Kawashima, Eur. Phys. J. B **9**, 233 (1999).

[60] R. H. Swendsen and J.-S. Wang, Phys. Rev. Lett. **58**, 86 (1987).

[61] J. M. Kosterlitz and D. J. Thouless, J. Phys. C **6**, 1181 (1973).

[62] J. M. Kosterlitz, Phys. Rev. Lett. **37**, 1577 (1976).

[63] P. Minnhagen, Phys. Rev. Lett. **54**, 2351 (1985).

[64] P. Minnhagen, Phys. Rev. B **32**, 3088 (1985).

[65] H. Weber and P. Minnhagen, Phys. Rev. B **37**, 5986 (1988).

[66] R. Kubo, J. Phys. Soc. Jpn. **12**, 570 (1957).

[67] G. De Filippis, V. Cataudella, A. de Candia, A. S. Mishchenko, and N. Nagaosa, Phys. Rev. B **90**, 014310 (2014).

[68] A. Fragner, M. Göppl, J. M. Fink, M. Baur, R. Bianchetti, P. J. Leek, A. Blais, and A. Wallraff, Science **322**, 1357 (2008).

[69] M. H. Devoret *et al.*, *Les Houches, Session LXIII* (Elsevier, Amsterdam, 1995).

[70] A. M. Zagoskin, *Quantum Engineering: Theory and Design of Quantum Coherent Structures* (Cambridge University Press, Cambridge, England, 2011).

[71] Following Devoret [69], the Hamiltonian $\omega_0 a^\dagger a + \sum_{i=1}^{\infty} [(p_i^2/2M_i) + (k_i/2)(x - x_i)^2]$ represents a lossy LC circuit, i.e., an LC circuit, with capacitance C_0 and inductance L_0 such that $\omega_0^2 = 1/C_0 L_0$, in the presence of a dissipative element replaced by an infinite number of purely reactive elements, where $k_i = 1/L_i$ and $M_i = C_i$ (in this case x and x_i are fluxes). The conductance G can be expressed in terms of the spectral density: $G = 2\pi\omega_0 C_0 J(\omega)/\omega = \pi\alpha_{\text{cav}}\omega_0 C_0$. Following Ref. [20], $C_0 = 2I_{zpf}^2/\hbar\omega_0^2$, with $\omega_0/2\pi \simeq 6$ GHz and I_{zpf}, the zero point fluctuations in the current, of order of tens of nanoamperes. The resistance $R = 1/G$ turns out to be $R = (0.24/\alpha_{\text{cav}})$ $k\Omega$. See Supplemental Material [39] for the circuit diagram.